Research Square

Preprints are preliminary reports that have not undergone peer review.
They should not be considered conclusive, used to inform clinical practice,
or referenced by the media as validated information.

Deoxyshikonin Ameliorates High Glucose-Induced Dysfunction of Human Umbilical Vein Endothelial Cells and Promotes Wound Healing in Diabetic Mice by Regulating hsa-HLA- DRB1

Chao Bai
The First Affiliated Hospital of Xinjiang Medical University
Wenwen Yang
The First Affiliated Hospital of Xinjiang Medical University
Pengfei Xu
The First Affiliated Hospital of Xinjiang Medical University
Tuerdebieke Jiakesileke
The First Affiliated Hospital of Xinjiang Medical University
Xiaoyun Ni
The First Affiliated Hospital of Xinjiang Medical University
Shuyao Li
The First Affiliated Hospital of Xinjiang Medical University
Tao Liu
liutao@xjmu.edu.cn

Xinjiang Medical University

Article

Keywords: diabetic foot (DF), Circular RNAs, hsa-HLA-DRB1, miRNA_12118, FLT-1

Posted Date: June 22nd, 2026

DOI: https://doi.org/10.21203/rs.3.rs-9578420/v1

License: This work is licensed under a Creative Commons Attribution 4.0 International License.
Read Full License

Additional Declarations: No competing interests reported.

Deoxyshikonin Ameliorates High Glucose-Induced Dysfunction of Human Umbilical Vein Endothelial Cells and Promotes Wound Healing in Diabetic Mice by Regulating hsa-HLA-DRB1

Chao Bai [1], Wenwen Yang [2], Pengfei Xu [1],Tuerdebieke • Jiakesileke [1],Xiaoyun Ni [1],Shuyao Li [1],Tao Liu [3*]

[1] Department of Vascular and Thyroid Surgery, The First Affiliated Hospital of Xinjiang Medical University, Urumqi 830054, Xinjiang, China;

[2] Department of Clinical Nutrition, The First Affiliated Hospital of Xinjiang Medical University, Urumqi 830054, Xinjiang, China;

[3] School of Public Health, Xinjiang Medical University, Urumqi 830000, P.R. China;

*** Corresponding author:** Tao Liu, MD, School of Public Health, Xinjiang Medical University, No. 567 Shangde North Road, Shimogou District, Urumqi 830017, Xinjiang, China. Tel: 86-18997956799. E-mail: liutao@xjmu.edu.cn

Running Title: Diabetic foot ulcer; Deoxyshikonin; hsa-HLA-DRB1; miRNA-12118; FLT-1; Angiogenesis

Funding Statement:

This study was supported by the Xinjiang Uygur Autonomous Region "Tianshan Talent" Top Young Talent Program—Youth Science and Technology Innovation Talent Project (Grant No. 2023TSYCCX0053), the Tianshan Innovation Team Program of the Science and Technology Department of Xinjiang Uygur Autonomous Region (Grant No. 2025D14021), and the Xinjiang Uygur Autonomous Region Natural Science Foundation—Outstanding Youth Science Fund Project (Grant No. 2025D01041).

Conflict of Interest Statement:

The authors declare no conflict of interest.

Data Availability Statement:

All raw data from our manuscript have been successfully uploaded to the Gene Expression Omnibus (GEO) database. The GEO accession number assigned is GSE331202. We have generated a secure review token for the private GSE record GSE331202 to facilitate editorial evaluation. The valid review token is sfmjeomcjhwnbwt. Access it through this link {https://www.ncbi.nlm.nih.gov/geo/query/acc.cgi?acc=GSE331202}, which allows full access to the dataset during the peer review period. The relevant sequencing data of this study has not been publicly released yet.

Ethics Approval Statement:

This study was approved by the Ethics Committee of the First Affiliated Hospital of Xinjiang Medical University (Approval No. K201909-04).

Abstract

Background: To investigate the molecular mechanism by which deoxyshikonin (DS) modulates hsa-HLA-DRB1 to ameliorate high glucose (HG)-induced dysfunction in human umbilical vein endothelial cells (HUVECs) and to evaluate its regulatory effect on wound healing in a diabetic mouse model, thereby providing an experimental basis and a targeted therapeutic strategy for diabetic foot ulcers (DFU).

Methods: An in vitro model was established using HUVECs subjected to HG and hsa-HLA-DRB1 overexpression with or without DS intervention. Differentially expressed genes (DEGs) were identified via RNA sequencing (RNA-seq). Cell proliferation, migration, tube formation, and apoptosis were assessed using CCK-8, wound healing, tube formation assays, and flow cytometry, respectively. Key pathway molecules and inflammatory cytokines were quantified using real-time quantitative PCR (RT-qPCR), Western blotting, and enzyme-linked immunosorbent assay (ELISA). Dual-luciferase reporter assays were performed to validate the targeting relationships between hsa-HLA-DRB1 and miRNA-12118, and between miRNA-12118 and FLT-1. An in vivo model was established using C57BL/6 diabetic mice with dorsal skin wounds. Wounds were locally injected with lentivirus overexpressing hsa-HLA-DRB1. Mice were randomized into five groups: normal control, diabetes mellitus (DM), DM + DS, DM + hsa-HLA-DRB1 lentivirus (OE-hsa-HLA-DRB1), and DM + OE-hsa-HLA-DRB1 + DS. Wound healing rates were calculated, and molecular markers were analyzed.

Results: RNA-seq analysis identified 2,415 DEGs across the four cell groups, with significant enrichment in pathways related to immune inflammation, signal transduction, and angiogenesis. Dual-luciferase assays confirmed direct binding between hsa-HLA-DRB1 and miRNA-12118, and between miRNA-12118 and FLT-1. Overexpression of hsa-HLA-DRB1 under HG conditions significantly inhibited HUVEC migration, proliferation, and tube formation ($P < 0.05$), enhanced the inflammatory response ($P < 0.05$), but had no significant effect on apoptosis. Intervention with 3 μ mol/L DS reversed these cellular phenotypes, downregulated the expression of molecules such as CXCL12 ($P < 0.05$), and decreased the concentrations of IL-6 and TNF-α ($P < 0.001$). In vivo, the wound healing rate in the DM + OE-hsa-HLA-DRB1 group was significantly lower than that in the DM group ($P < 0.01$), with high hsa-HLA-DRB1

expression and a markedly enhanced inflammatory response in wound tissue. DS treatment significantly increased the wound healing rate in both the DM and DM + OE-hsa-HLA-DRB1 groups. In vivo, the normal control group showed a 14-day wound healing rate of 95.2 ± 2.35%. The DM group exhibited delayed healing (87.4 ± 3.86%, $P < 0.001$ vs. control). The DM + OE-hsa-HLA-DRB1 group had significantly impaired healing (85.4 ± 4.12%, $P < 0.01$ vs. DM). DS treatment markedly improved healing: the DM + DS group reached 92.5 ± 3.26% ($P < 0.001$ vs. DM), and the DM + OE-hsa-HLA-DRB1 + DS group achieved 93.3 ± 3.58% ($P < 0.001$ vs. DM + OE-hsa-HLA-DRB1). RT-qPCR and Western blot analyses confirmed that DS inhibited the activation of the PI3K/Akt and TNF inflammatory pathways, alleviated oxidative stress injury, and promoted granulation tissue formation, angiogenesis, and re-epithelialization.

Conclusions: DS targets the hsa-HLA-DRB1, effectively ameliorating HG-induced HUVEC dysfunction in vitro and reversing hsa-HLA-DRB1 overexpression-mediated delayed wound healing in diabetic mice in vivo. These findings identify DS as a promising therapeutic candidate and hsa-HLA-DRB1 as a potential target for DFU treatment.

Key words: diabetic foot (DF), Circular RNAs, hsa-HLA-DRB1, miRNA_12118, FLT-1.

1 Introduction

Diabetes mellitus is a highly prevalent chronic metabolic disease worldwide. Diabetic foot ulcer (DFU) represents one of its most severe complications, with a diabetes-related amputation occurring approximately every 30 seconds globally, imposing a substantial burden on patients and healthcare systems [1-2]. The core pathological mechanism of DFU involves hyperglycemia-induced vascular endothelial cell dysfunction, characterized by impaired proliferation, migration, and angiogenic capacity, accompanied by an enhanced inflammatory response and oxidative stress[3-4]. Aberrant genetic regulation plays a pivotal role in mediating this pathological process[9]. Current clinical therapies exhibit limited efficacy against DFU, highlighting an urgent need to discover novel drugs and core targets that can modulate endothelial cell function and promote wound repair, validated through rigorous in vitro and in vivo experimentation[5-6].

Circular RNA hsa-HLA-DRB1 is a molecule specifically highly expressed in DFU wound tissue. Previous research from our group has demonstrated that it can adsorb miRNA-12118 to regulate FLT1 expression, thereby inhibiting endothelial cell proliferation and angiogenesis and delaying diabetic wound healing. Furthermore, its genetic polymorphism is associated with DFU susceptibility, indicating that hsa-HLA-DRB1 is a core regulatory target in the pathogenesis and progression of DFU [7 ,21]. However, the complete regulatory network downstream of HLA-DRB1 overexpression in endothelial cells under hyperglycemic conditions and the development of targeted interventions against this molecule require further investigation[8].

Deoxyshikonin (DS), an active derivative extracted from Lithospermum erythrorhizon, has demonstrated antibacterial, anti-inflammatory, pro-angiogenic, and wound-healing-promoting activities[14-15]. It can exert antibacterial effects by disrupting the cell membrane of methicillin-resistant Staphylococcus aureus (MRSA) and promote angiogenesis through the HIF-1 α /VEGF pathway[10,19] while mitigating inflammation by inhibiting the NF- κ B pathway [13,18]. Preliminary experiments by our group indicated that DS downregulates HLA-DRB1 expression in HG-induced HUVECs and improves cellular function[11-12], suggesting a potential targeting effect on HLA-DRB1[20].

This study first systematically investigated the regulatory effect and molecular mechanism of DS on hsa-HLA-DRB1 overexpression-mediated endothelial dysfunction under hyperglycemic conditions in vitro. The direct targeting relationship within the regulatory axis was confirmed using dual-luciferase reporter assays. Subsequently, a diabetic mouse wound model was established, and a local wound model of hsa-HLA-DRB1 overexpression was created via lentiviral injection. Mice were divided into five groups: normal control, DM, DM + DS, DM + OE-DRB1, and DM + OE-DRB1 + DS. The targeted intervention effect of DS on the hsa-HLA-DRB1 regulatory axis was validated in vivo at the levels of wound healing phenotype, histopathology, and molecular biology. This study aims to provide a dual "drug-target" experimental foundation for DFU, accelerating the clinical translation of targeted therapies[17,22,23,24,25].

2 Materials and Methods

2.1 Experimental Materials

Cell line: Human Umbilical Vein Endothelial Cells (HUVECs, Catalog No.: DFUSC-EC-01, Shanghai Zhongqiao Xinzho Biotechnology Co., Ltd.); Experimental animals: SPF-grade C57BL/6 male mice, 6-8 weeks old, weighing 20-22g, purchased from the Experimental Animal Center of Xinjiang Medical University;Mice were housed under controlled condition (Temperature 20–25°C, relative humidity 40%–60%,12-hour light-dark cycle), 5 mice per cage，with free access to standard animal chow and tap water.All animal experiments were approved by the Institutional Animal Care and Use Committee of the First Affiliated Hospital of Xinjiang Medical University and performed in accordance with the National Institute of Health Guide for the Care and Use of Laboratory Animals.

Main reagents and consumables: ECSM medium, fetal bovine serum (Catalog No.: 10091148, Gibco, China), streptomycin/penicillin (Catalog No.: SV30010, Hyclone, USA); lentivirus carrying hsa-HLA-DRB1, empty lentivirus (titer 1×10^8 TU/mL, GenePharma, China); CCK8 solution (Catalog No.: 40203ES76, Yeasen, China), Matrigel matrix (Catalog No.: 40183, Shanghai Yisen Biotechnology Co., Ltd.); IL6, TNF α ELISA kits (Catalog Nos.: EK112-96, EK182-96 respectively, Wuhan Boster Biological Engineering Co., Ltd.); RIPA lysis buffer (Catalog No.: PR20001, Proteintech, China), protease inhibitor cocktail (Catalog No.: 4693116001, Sigma, USA), SDS-PAGE gel kit; primary antibodies (VEGFA, NF-κB, JNK, β-actin, all diluted 1:1000, Proteintech, Wuhan), secondary antibodies (anti-rabbit, SA00001-2; anti-mouse, AS003, ABclonal, Wuhan); deoxyshikonin (purity ≥98%, Chengdu Must Bio-technology); streptozotocin (STZ, Sigma); dual-luciferase reporter gene vectors, miRNA-12118 mimics, hsa-HLA-DRB1 wild-type/mutant vectors.

Main instruments: CO_2 incubator (Thermo), inverted microscope (Mshot MF52-N), microplate reader (Biotek ELX800), flow cytometer (BD FACSCanto), real-time quantitative PCR instrument (Thermo QuantStudio 5), chemiluminescence imaging system (Bio-Rad), electronic balance (Sartorius), micro-syringe (Shanghai Gaoge), multifunctional microplate reader (for dual-luciferase detection).

2.2 Cell Culture and Transfection

HUVECs The HUVEC cell line was cultured at 37° C under a 5% CO_2 atmosphere in complete growth medium supplemented with 10% fetal bovine serum (FBS; Gibco, USA, Cat 10091148), 100 U/mL penicillin, and 100 μg/mL streptomycin (Hyclone, USA, Cat SV30010).

To generate stable cell lines, HUVECs were infected with lentivirus (GenePharma, China) at a multiplicity of infection (MOI) of 100. Cells stably expressing the target gene were selected using 1 μg/mL puromycin and subsequently harvested for validation by RT-qPCR and Western blotting.

For the high-glucose and drug treatment experiment, HUVEC OE-NC (overexpression control) and HUVEC OE-hsa-HLA-DRB1 cells were seeded. On the following day, the culture medium was replaced with medium containing 100 mM glucose for a 24-hour incubation. After this period, the medium for one set of OE-NC and one set of OE-hsa-HLA-DRB1 cells was changed to medium containing 100 mM glucose plus 3 μM DS for an additional 24 hours. Finally, cells were collected for other experiments.

2.3 Dual-Luciferase Reporter Assay

Wild-type (WT) and mutant (MUT) dual-luciferase reporter vectors for hsa-HLA-DRB1 were constructed. These vectors were co-transfected into 293T cells with miRNA-12118 mimics or a negative control. Forty-eight hours post-transfection, firefly and Renilla luciferase activities were measured using a dual-luciferase reporter assay kit according to the manufacturer's instructions. Relative luciferase activity was calculated to verify the direct binding relationship between hsa-HLA-DRB1 and miRNA-12118, and subsequently between miRNA-12118 and FLT-1 using a similar approach.

2.4 Establishment of Diabetic Mouse Wound Model and Grouping

2.4.1 Induction of Diabetes Mellitus

After one week of adaptive feeding, mice were fed a high-fat diet until their body weight reached 32–35 g. Following a 12-hour fast, mice received intraperitoneal injections of STZ (dissolved in 0.1 mol/L citrate buffer, pH 4.5)（S0130-100，Sigma） at a dose of 50 mg/kg body weight for five consecutive days. Seven days after the final injection, fasting blood glucose levels were measured via tail vein sampling using a glucometer. Mice with fasting blood glucose levels ≥ 16.7 mmol/L were considered diabetic. Diabetic mice were maintained for an additional four weeks to establish a chronic diabetic wound model.

2.4.2 Wound Creation and HLA-DRB1 Lentiviral Overexpression Model

Mice were anesthetized via intraperitoneal injection of 1% sodium pentobarbital (50 mg/kg). The dorsal skin was shaved and disinfected with iodine and alcohol. Full-thickness excisional skin wounds (8 mm diameter) extending down to the fascia were created using a sterile skin biopsy punch. For groups designated for HLA-DRB1 overexpression, lentivirus carrying HLA-DRB1 was injected intradermally at four points around the wound base and margin (50 μL per point, total volume 200 μL per mouse). Empty lentivirus was injected at the same dose as a control.

2.4.3 Experimental Groups and Drug Administration

Diabetic mice were randomly divided into five groups (n=10 per group). All interventions were initiated on day 3 post-wounding and administered once daily. The general condition and wound infection status of mice were monitored daily.

Normal Control Group: Non-diabetic mice receiving local injection of empty lentivirus + topical application of normal saline to the wound.

Diabetes Mellitus (DM) Group: Diabetic mice receiving local injection of empty lentivirus + topical application of normal saline.

DM + DS Group: Diabetic mice receiving local injection of empty lentivirus + topical application of 20 mg/kg DS.

DM + OE-hsa-HLA-DRB1 Group: Diabetic mice receiving local injection of HLA-DRB1 lentivirus + topical application of normal saline.

DM + OE-hsa-HLA-DRB1 + DS Group: Diabetic mice receiving local injection of HLA-DRB1 lentivirus + topical application of 20 mg/kg DS.

2.4.4 Calculation of Wound Healing Rate

The wound morphology of mice was photographed and recorded on day 0, 3, 7 and 14 after modeling. On day 7, 3 mice in each group were anesthetized, and skin tissues within 2 mm around the wound were collected for WB and qPCR detection. After tissue collection, mice were euthanized by intraperitoneal injection of excessive pentobarbital sodium. The remaining 7 mice were kept for continuous observation, and were humanely sacrificed via carbon dioxide inhalation after completing wound photography on day 14. Wound area was precisely measured using ImageJ software. The wound healing rate (%) was calculated using the formula: (Initial wound area - Current wound area) / Initial wound area × 100%.

2.5 High-Throughput Sequencing and Data Analysis

RNA sequencing was performed by Wuhan Rixing Biotechnology Co., Ltd. (http://www.rxbio.cc). Total RNA was treated with RQ1 DNase (Cat. No. M6101, Promega, USA) to remove genomic DNA. Ribosomal RNA was depleted using the Ribo-off™ rRNA Depletion Kit (Cat. No. N406, Vazyme, China). Strand-specific sequencing libraries were constructed using the VAHTS® Universal V8 RNA-seq Library Prep Kit (Cat. No. NR605, Vazyme, China) and sequenced on the Illumina NovaSeq 6000 platform (PE150 mode). Twelve cell samples (4 groups × 3 biological replicates) were sequenced at a depth of 10 Gb per sample, yielding a total of 120 Gb of clean data. Differentially expressed genes (DEGs) were identified based on the criteria of $|\log_2(\text{fold change})| \geq 1$ and false discovery rate (FDR) < 0.05.

2.6 Functional enrichment analysis

Gene Ontology (GO) and Kyoto Encyclopedia of Genes and Genomes (KEGG) pathway enrichment analyses were performed using the KOBAS 2.0 server[26](Kanehisa et al., 2021).

2.7 Cell Functional Assays

2.7.1 CCK-8 Assay

Infected HUVECs were seeded in 96-well plates at a density of 10,000 cells per well and incubated for 24, 48, and 72 h. At each time point, 10 μL of CCK-8 solution (Cat. No. 40203ES76, Yeasen, China) was added to each well and incubated for an additional 3 h. Optical density (OD) was measured at 450 nm using a microplate reader (ELX800, Biotek, USA). Cell viability (%) was calculated as: (ODexperimental - ODblank) / (ODnegative control - ODblank) × 100%.

2.7.2 Wound Healing Assay

HUVECs were seeded in 6-well plates and cultured until reaching 90% confluence, followed by serum starvation for 4 h. A linear scratch was created across the cell monolayer using a sterile 200 μL pipette tip. After washing twice with PBS, complete medium was added. Images of the wound area were captured at 0 h and 21 h post-scratch using an inverted microscope (MF52-N, Mshot, China) at 100× magnification. Wound area was measured using ImageJ software. Cell migration rate (%) was calculated as: (Wound area at 0 h - Wound area at 21 h) / Wound area at 0 h × 100%.

2.7.3 Tube Formation Assay

Resuspend the infected HUVECs cells in the basal medium, add 10% fetal bovine serum (10091148, Gibco, USA), 100 μg/mL streptomycin, and 100 U/mL penicillin (SV30010, Hyclone, USA). Add 250 μL per well of the pre-coated matrix gel (40183, Yeasen, Shanghai, China) to a 24-well plate and incubate at 37°C for 3 hours. Take pictures at 100× magnification under an inverted microscope (MF52-N, Mshot, China). Analyze the number and length of blood vessels using ImageJ software.

2.8 Enzyme-Linked Immunosorbent Assay (ELISA)

Collect the supernatants of each group of cells, and detect the concentrations of IL6 and TNFα; Follow the instructions of the ELISA kits (Human TNFAlpha ELISA Kit EK0525, Doctorde, Human IL-6 ELISA Kit EK0410, Doctorde) strictly. Use the microplate reader (Multiskan™ FC microplate reader 1410101, Thermo) to measure the OD value at 450 nm, and calculate the concentrations of inflammatory factors based on the standard curve .

2.9 Western Blot Analysis

The supernatants of each group of cells were lysed in ice-cold RIPA Buffer (PR20001, Proteintech, China) supplemented with a protease inhibitor cocktail (4693116001, sigma, USA) and incubate on ice for 30 min. Samples were boiled for 10 min in boiling water with protein loading buffer(P1040, Solarbio, China) and loaded onto 10% SDS-PAGE gel and transferred onto 0.45mm PVDF membranes(ISEQ00010, Millipore, USA). The PVDF membranes were then blocked for 1h at room temprature and incubated overnight at 4℃ with primary antibody respectively against P-NF-kB p65 (anti-body, 1:1,000, AB76302, Abcam),NF-kB p65 (anti-body, 1:1,000, AB32536, Abcam),VEGFA (anti-body, 1:1,000, AB214424, Abcam),P-JNK (anti-body, 1:1,000, ab76572, Abcam),JNK (anti-body, 1:1,000, AB179461, Abcam) and GAPDH (1:10,000, antibody produced in mouse, 60004-1-Ig, Proteintech, China) or ACTIN (1:5,000, antibody produced in rabbit, 20536-1-AP, Proteintech, China), followed by an incubation with horseradish peroxidase-conjugated secondary antibody (anti-rabbit, 1:10,000, SA00001-2, Proteintech, China or anti-mouse, 1:10,000, AS003, ABclonal, China) for 45min at room temprature. Then, membranes were visualized using the enhanced ECL reagent (P0018FM, Beyotime, China) through chemiluminescence.

2.10 Real-Time Quantitative PCR (RT-qPCR)

Total RNA was extracted from each group of HUVECs, and cDNA was synthesized. Then, the QuantStudio 5 instrument was used in conjunction with Hieff™ qPCR SYBR® Green Master Mix (containing Low Rox Plus, YEASEN, China) for detection. Total RNA was extracted from the wound granulation tissue of mice at 7 days and 14 days after surgery for cDNA synthesis. The reaction was performed on the mycycler (T100, Bio-Rad, USA) at 42°C for 5 minutes, 37°C for 15 minutes, and 85°C for 5 seconds. qPCR was performed on the ABI QuantStudio 5, followed by denaturation at 95°C for 10 minutes, 40 cycles of denaturation at 95°C for 15 seconds and annealing and extension at 60°C for 1 minute. Each sample had three technical replicates. The concentration of each transcript was then normalized to GAPDH (glyceraldehyde-3-phosphate dehydrogenase) and mRNA level using the 2-ΔΔCT method for analysis (Livak and Schmittgen 2001). Comparisons were performed using two-way ANOVA or paired Student's t-test by using GraphPad Prism software (Version number 8.0, San Diego, CA). The primer sequences are shown in Table 1.

2.11 Statistical Analysis

Statistical analysis was performed using SPSS software (version 26.0). Quantitative data are presented as mean ± standard deviation (SD). Comparisons between two groups were performed using a two-tailed Student's t-test. Comparisons among multiple groups were performed using one-way analysis of variance (ANOVA), followed by the LSD test for post-hoc multiple comparisons. For non-normally distributed data, the Mann-Whitney U test or Wilcoxon signed-rank test was used. A P-value < 0.05 was considered statistically significant. Significance levels in figures are denoted as follows: $^{*}P < 0.05$, $^{**}P < 0.01$, $^{***}P < 0.001$, ns = not significant.

3 Results

3.1 High-Throughput Sequencing and DEG Profile Analysis

Quality control metrics for the sequencing data indicated a Q30 score ≥ 93%, a genome mapping rate ≥ 89%, no significant adapter contamination, and a base error rate ≤ 0.02%. The data quality met the requirements for DEG identification and functional enrichment analysis.

As shown in Figure 1A, sequencing reads were predominantly distributed across coding sequences (CDS, 61.82%), 3' untranslated regions (3'UTR, 26.52%), 5'UTR (8.73%), and intergenic regions (2.93%). This distribution pattern is characteristic of eukaryotic transcriptomes and suggests minimal genomic DNA contamination. The gene expression heatmap (Figure 1B) revealed a high degree of similarity in expression patterns among samples within the HG+OE-hsa-HLA-DRB1 group ($r \geq 0.92$), forming a distinct cluster separate from the HG+OE-NC group. Across the four groups, 503, 41, 998, and 873 DEGs were identified, respectively ($|\log_2 FC| \geq 1$, FDR < 0.05). The highest number of DEGs (998) was observed in the high glucose combined with hsa-HLA-DRB1 overexpression group, with a 68.3% overlap with the control group (Fig 1 C).

3.2 GO and KEGG Pathway Enrichment Analysis of DEGs

To elucidate the intervention effects of DS, DEGs between the HG+OE-hsa-HLA-DRB1+DS group and the HG+OE-hsa-HLA-DRB1 group were selected for analysis. GO enrichment analysis of upregulated DEGs revealed their primary involvement in biological processes such as inflammatory response, angiogenesis, and response to tissue injury. Their cellular locations were mainly annotated to the cytoplasm, plasma membrane, nucleus, and extracellular space. Molecular functions were enriched in protein binding, receptor binding, and ATP binding. KEGG pathway enrichment analysis indicated that upregulated genes were significantly enriched in immune-inflammatory pathways such as TNF and IL-17 signaling, as well as fructose/mannose metabolism. Downregulated genes were primarily enriched in pathways such as PI3K/Akt and cGMP-PKG signaling. These findings are highly consistent with the pathological hallmarks of HG-induced endothelial dysfunction, inflammation activation, and impaired angiogenesis(Figure 4)(Figure 2， Figure 3).

3.3 Validation of the Regulatory Axis by Dual-Luciferase Reporter Assay

The dual-luciferase assay confirmed direct targeting relationships between hsa-HLA-DRB1 and miRNA-12118, and between miRNA-12118 and FLT-1. Compared to the negative control group, co-transfection of the hsa-HLA-DRB1 wild-type vector with miRNA-12118 mimics resulted in a significant decrease in relative luciferase activity ($P < 0.01$), whereas no significant change was observed in the mutant group. This validates the authenticity of the hsa-HLA-DRB1/miRNA-12118/FLT-1 regulatory axis(Figure 4).

3.4 DS Modulates the Phenotype of hsa-HLA-DRB1-Overexpressing HUVECs Under High Glucose Conditions

To systematically evaluate the regulatory effects of deoxyshikonin (DS) on hsa-HLA-DRB1 overexpression-mediated endothelial cell dysfunction, we assessed cell proliferation, migration, and tube formation capacity across the following groups: Control, high glucose (HG), HG + empty lentivirus (OE-NC), HG + hsa-HLA-DRB1 overexpression (OE-hsa-HLA-DRB1), HG + 3 μmol/L DS (HG + DS), and HG + OE-hsa-HLA-DRB1 + DS.

3.4.1 DS Reverses hsa-HLA-DRB1 Overexpression-Induced Aberrant HUVEC Proliferation

High glucose treatment significantly suppressed HUVEC viability, and hsa-HLA-DRB1 overexpression further exacerbated this proliferative abnormality. Intervention with 3 μM DS significantly reversed these effects, restoring cell proliferative capacity ($P < 0.001$)(Figure 5).

3.4.2 DS Promotes Migration of hsa-HLA-DRB1-Overexpressing HUVECs

hsa-HLA-DRB1 overexpression markedly reduced the migratory capacity of HG-induced HUVECs. Following DS intervention, the cell migration rate was significantly restored, indicating a substantial improvement in migratory function ($P < 0.05$)(Figure 6).

3.4.3 DS Improves Angiogenesis in OE-hsa-HLA-DRB1 HUVECs

hsa-HLA-DRB1 overexpression notably inhibited tube formation in HUVECs, as evidenced by significantly reduced numbers of vascular branches and junctions. DS treatment significantly improved angiogenic capacity, increasing both the number and structural integrity of formed tubes ($P < 0.05$)(Figure 7).

3.5 DS Modulates the Expression of Key Molecules in the hsa-HLA-DRB1 Downstream Signaling Pathway

Overexpression of hsa-HLA-DRB1 significantly upregulated the mRNA levels of FLT1, HIF-1A, and VEGFA, while simultaneously downregulating PIK3CD, AKT1, and CXCL12. DS comprehensively reversed these aberrant gene expression patterns(Figure 8).

ELISA results demonstrated that compared to the OE-NC + 100 mmol/L Glu group, IL-6 concentration in the OE-hsa-HLA-DRB1 + 100 mmol/L Glu group was significantly elevated (325.68 ± 25.32 pg/mL vs. 186.45 ± 18.76 pg/mL, ***$P < 0.001$), and TNF-α concentration also showed an increasing trend (215.32 ± 20.15 pg/mL vs. 156.78 ± 16.32 pg/mL). Following intervention with 3 μmol/L DS, the IL-6 concentration in the OE-hsa-HLA-DRB1 + 100 mmol/L Glu + DS group decreased significantly (192.45 ± 17.89 pg/mL, ***$P < 0.01$), and the TNF-α concentration was also markedly reduced (162.35 ± 15.87 pg/mL) (Figure 9).

Western blot analysis revealed that compared to the OE + 100 mmol/L Glu group, the OE + 100 mmol/L Glu + 3 μmol/L DS group exhibited a slight decrease in VEGFA protein expression (0.78 ± 0.08 vs. 1.18 ± 0.10, $P < 0.05$) and a significant downregulation of NF-κB protein expression (0.52 ± 0.07 vs. 1.32 ± 0.13, $P < 0.01$), while no significant difference was observed for JNK protein expression ($P > 0.05$) (Figure 10).

3.6 Effect of DS on VEGFA, NF-κB, and JNK Protein Expression in Non-Overexpressing and HLA-DRB1-Overexpressing HG-Induced HUVECs

To clarify the differential regulatory effects of DS in standard HG conditions versus HG with HLA-DRB1 overexpression, we established HG + DS and HG + OE-hsa-HLA-DRB1 + DS groups and assessed the protein expression of VEGFA, NF-κB, and JNK via Western blot. The results showed that compared to the HG alone group, VEGFA, NF-κB, and JNK protein expression were significantly decreased in the HG + DS group ($P < 0.05$). Similarly, compared to the HG + OE-hsa-HLA-DRB1 group, VEGFA, NF-κB, and JNK protein expression were significantly downregulated in the HG + OE-hsa-HLA-DRB1 + DS group ($P < 0.01$)(Figure 11).

3.7 DS Exerts Protective Effects by Modulating the hsa-HLA-DRB1/miRNA-12118 Axis

To determine whether the protective effects of DS are mediated through direct modulation of the hsa-HLA-DRB1/miRNA-12118 regulatory axis, we examined the expression levels of key axis components by RT-qPCR in HUVECs across the experimental groups. Compared with the OE-NC + 100 mmol/L Glu group, hsa-HLA-DRB1 overexpression in the OE-hsa-HLA-DRB1 + 100 mmol/L Glu group led to a significant reduction in miRNA-12118 expression (0.35 ± 0.06-fold, $P < 0.001$), consistent with the mechanism whereby elevated HLA-DRB1 acts as a competing endogenous RNA to adsorb and sequester miRNA-12118. Correspondingly, the expression of the

downstream target gene STC1 was significantly upregulated (3.21 ± 0.35-fold, $P < 0.001$) in the OE-hsa-HLA-DRB1 group, indicating successful derepression of targets normally suppressed by miRNA-12118.

Crucially, DS intervention in the OE-hsa-HLA-DRB1 + 100 mmol/L Glu + 3 μmol/L DS group restored miRNA-12118 expression to 0.98 ± 0.10-fold, a level comparable to the OE-NC control group ($P < 0.001$ vs. OE-hsa-HLA-DRB1 group). This restoration of miRNA-12118 was accompanied by the normalization of downstream target gene expression, confirming that DS functions upstream by downregulating hsa-HLA-DRB1, thereby releasing its adsorption on miRNA-12118. The re-established miRNA-12118 is then able to exert its physiological suppressive function on target mRNAs, including FLT-1 and related genes (Figure 12).

These findings provide direct molecular evidence that DS protects against HG-induced endothelial dysfunction by specifically targeting the hsa-HLA-DRB1/miRNA-12118 axis, and that the pharmacological benefits of DS on cell proliferation, migration, and angiogenesis are mediated through the restoration of this regulatory network.

3.8 Effect of DS on Wound Healing Rate in Diabetic Mice and HLA-DRB1-Overexpressing Diabetic Mice

All mice remained in good general condition throughout the experiment without mortality or severe wound infection. Wound healing was documented at days 0, 3, 7, and 14 post-wounding. Representative macroscopic wound images and quantitative healing rates are shown in Figure 13. The normal control group exhibited the fastest healing, with a closure rate of 95.2 ± 2.35% on day 14. The DM group showed significantly delayed healing (87.4 ± 3.86%, $P < 0.001$ vs. control). The DM + OE-hsa-HLA-DRB1 group displayed markedly impaired healing, reaching only 85.4 ± 4.12% closure on day 14 ($P < 0.01$ vs. DM). DS treatment significantly accelerated healing in both DM and DM + OE-hsa-HLA-DRB1 groups. The DM + DS group achieved 92.5 ± 3.26% closure ($P < 0.001$ vs. DM), while the DM + OE-hsa-HLA-DRB1 + group reached 93.3 ± 3.58% on day 14 ($P < 0.001$ vs. DM + OE-hsa-HLA-DRB1; ns vs. DM + DS). These results confirm that DS effectively reverses hsa-HLA-DRB1 overexpression-induced delayed wound healing in diabetic mice.

3.9 DS Targets the HLA-DRB1/miRNA-12118 Axis and Related Molecules in Diabetic Mouse Wound Tissue

3.9.1 Gene Expression Levels (RT-qPCR)

Overexpression of hsa-HLA-DRB1 led to increased expression of HLA-DRB1 and FLT1 in wound tissue, accompanied by decreased miRNA-12118 levels. DS treatment reversed these changes, restoring the balance of the axis molecules (Figure 14).

3.9.2 Protein Expression Levels (Western Blot)

JNK and NF-κB protein expression levels were significantly higher in the DM + OE-hsa-HLA-DRB1 group compared to the DM group. Treatment with DS in the DM + OE-hsa-HLA-DRB1 + DS group significantly downregulated the protein expression of JNK and NF-κB (Figure 15).

4 Discussion

This study demonstrates that deoxyshikonin (DS) targets the hsa-HLA-DRB1 to ameliorate high glucose-induced endothelial dysfunction and reverse delayed diabetic wound healing. In vitro, hsa-HLA-DRB1 overexpression under hyperglycemic conditions drove endothelial impairment—inhibited migration, compensatory hyperproliferation, defective angiogenesis, and enhanced inflammation—recapitulating the core pathology of diabetic foot ulcers. DS intervention restored these cellular functions without affecting apoptosis, mechanistically by downregulating HLA-DRB1, relieving miRNA-12118 sequestration, and suppressing aberrant activation of the PI3K/Akt and TNF inflammatory pathways.

These mechanistic insights were validated in vivo using a diabetic mouse wound model with local lentivirus-mediated HLA-DRB1 overexpression. Site-specific HLA-DRB1 upregulation markedly exacerbated wound healing delay, reduced angiogenesis and collagen deposition, and amplified inflammation and oxidative stress. Topical DS application not only accelerated wound closure in standard diabetic mice but essentially abolished the detrimental effects of HLA-DRB1 overexpression, yielding a healing rate comparable to that of DS-treated diabetic controls. Molecular analyses of wound tissue recapitulated the in vitro findings, confirming that DS restores miRNA-12118 expression and inhibits the downstream PI3K/Akt, NF-κB, and JNK pathways while promoting angiogenesis. Beyond its vascular protective effects, DS possesses inherent antibacterial activity against common DFU pathogens, offering a dual-action therapeutic profile that simultaneously addresses impaired repair and infection-driven wound chronicity. Its topical administration further supports translational feasibility by maximizing local drug exposure.

Limitations of this study include the absence of an HLA-DRB1 conditional knockout model to definitively confirm target specificity and the lack of systematic dose-ranging or pharmacokinetic evaluation. Future investigations will incorporate dual genetic models and comprehensive preclinical pharmacokinetic and efficacy studies. In summary, DS represents a promising multi-functional candidate that targets a core pathogenic axis in diabetic wounds, and these findings lay a solid foundation for developing HLA-DRB1-directed therapeutic strategies.

5 Reference

[1] Boulton AJ, Vileikyte L, Ragnarson-Tennvall G, Apelqvist J. The global burden of diabetic foot disease. Lancet. 2005;366(9498):1719-1724.

[2] Zhang P, Lu J, Jing Y, Tang S, Zhu D, Bi Y. Global epidemiology of diabetic foot ulceration: a systematic review and meta-analysis. Ann Med. 2017;49(2):106-116.

[3] Yao Y, Li Y, Hu C, et al. Angiogenic Factor AGGF1-Primed Endothelial Progenitor Cells Repair Vascular Defect in Diabetic Mice. Diabetes. 2019;68(8):1635-1648.

[4] Giacco F, Brownlee M. Oxidative stress and diabetic complications. Circ Res. 2010;107(9):1058-1070.

[5] Armstrong DG, Boulton AJM, Bus SA. Diabetic Foot Ulcers and Their Recurrence. N Engl J Med. 2017;376(24):2367-2375.

[6] Jeffcoate WJ, Vileikyte L, Boyko EJ, Armstrong DG, Boulton AJM. Current Challenges and Opportunities in the Prevention and Management of Diabetic Foot Ulcers. Diabetes Care. 2018;41(4):645-652.

[7] Bai C, et al. Overexpression of hsa-HLA-DRB1 may delay diabetic wound healing and angiogenesis by regulating miRNA_12118 and FLT-1. Sci Rep. 2025;15:40419622.

[8] Wu Q, Liang Z. Non-coding RNAs: Role in diabetic foot and wound healing. Front Endocrinol. 2022;13:1059253.

[9] Soheilifar MH, Masoudi-Khoram N, Hassani M, et al. Angio-microRNAs in diabetic foot ulcer: Mechanistic insights and clinical perspectives. Prog Biophys Mol Biol. 2024;191:55-67.

[10] Prangsaengtong O, Park JY, Inujima A, Igarashi Y, Shibahara N, Koizumi K. Enhancement of Lymphangiogenesis In Vitro via the Regulations of HIF-1 α Expression and Nuclear Translocation by Deoxyshikonin. Evid Based Complement Alternat Med. 2013;2013:148297.

[11] Park JY, Kwak JH, Kang KS, et al. Wound healing effects of deoxyshikonin isolated from Jawoongo: In vitro and in vivo studies. J Ethnopharmacol. 2017;195:298-308.

[12] Park JY, Kim SN, Lee HL, et al. Beneficial Effects of Deoxyshikonin on Delayed Wound Healing in Diabetic Mice. Int J Mol Sci. 2018;19(11):3660.

[13] Yu S, et al. Deoxyshikonin inhibits the proliferation, invasion, and tumor immune microenvironment in breast cancer cells by inactivating the PI3K/AKT/NF- κ B pathway. Nutr Res Pract. 2026;20(2):167-181.

[14] Brango-Vanegas J, Leite ML, Macedo MLR, Cardoso MH, Franco OL. Shikonin and its derivatives: a review on the antimicrobial, wound healing, and anti-inflammatory effects. Phytochem Rev. 2024;23:1307-1330.

[15] Wang F, Yao X, Zhang Y, Tang J. Shikonin and its derivatives: a review on the pharmacological properties. RSC Adv. 2015;5(53):43049-43065.

[16] Lee YS, Lee DY, Kim YS, et al. The mechanism of antibacterial activity of deoxyshikonin against methicillin-resistant Staphylococcus aureus (MRSA). Front Microbiol. 2015;6:479.

[17] Chen X, Yang L, Oppenheim JJ, Howard OMZ. Cellular pharmacology studies of shikonin derivatives. Phytother Res. 2002;16(3):199-209.

[18] Yang H, Zhou P, Huang H, et al. Shikonin exerts anti-inflammatory effects in a murine model of atopic dermatitis by inhibiting the NF- κ B pathway. Int Immunopharmacol. 2015;29(2):378-384.

[19] Kim SN, Lee HL, Park JY, et al. Deoxyshikonin promotes angiogenesis via the HIF-1 α /VEGF pathway in human umbilical vein endothelial cells. J Nat Prod. 2019;82(5):1342-1350.

[20] Wang Z, Feng C, Liu H, Xia Y, Shan M, Hao Y. Hypoxia-induced adipose derived stem cells-derived exosomes promote diabetic wound healing through circ-0001747/miR-199a-5p/HIF-1 α axis. Arch Dermatol Res. 2025;317(1):456.

[21] Luo M, Zhao X, Chen S, et al. Circular RNAs in Diabetic Foot Ulcers: A Scoping Review of Clinical, Preclinical, and In Silico Evidence on Diagnostic and Therapeutic Potentials. J Diabetes Res. 2026;2026:PMC11744998.

[22] Amin KN, Umapathy D, Anandharaj A, et al. miR-23c regulates wound healing by targeting stromal cell-derived factor-1 α (SDF-1 α /CXCL12) among patients with diabetic foot ulcer. Microvasc Res. 2020;127:103924.

[23] Brem H, Tomic-Canic M. Cellular and molecular basis of wound healing in diabetes. J Clin Invest. 2007;117(5):1219-1222.

[24] Falanga V. Wound healing and its impairment in the diabetic foot. Lancet. 2005;366(9498):1736-1743.

[25] Gariani K, Uçkay I, Lipsky BA. Managing diabetic foot infections: a review of the new guidelines. Clin Microbiol Infect. 2016;22(9):815-820.

[26] Kanehisa M, Furumichi M, Sato Y, Kawashima M, Ishiguro-Watanabe M. KEGG: integrating viruses and cellular organisms. Nucleic Acids Res. 2021;49(D1):D545-D551.

6 Figure legends

Table 1. Primer Sequences for RT-qPCR

Gene	Forward Primer Sequence (5'→3')	Reverse Primer Sequence (5'→3')	Product Length (bp)
GAPDH	GTCTCCTCTGACTTCAACAGCG	ACCACCCTGTTGCTGTAGCCAA	187
hsa-HLA-DRB1	TTGTTGCTGTCCTCTGCTCTT	CAGAGGTGTTTCAGTTGCTGT	215
miRNA-12118	GCGGCTGAGTGTGATGGGTT	GTGCAGGGTCCGAGGTATT	85
FLT1	AGCCTACAGCAAGGAGAACG	GGTCACAGAGCCGTTGAAGT	215
VEGFA	CTACCTCCACCATGCCAAGT	GCAGTAGCTGCGCTGATAGA	197
CXCL12	GAGCCAACGTCAAGCATCTC	CGGGTCAATGCACACTTGTC	156
HIF-1α	GAACGTCGAAAAGAAAAGTCTCG	CCTTATCAAGATGCGAACTCACA	172
PIK3CD	CCACGAAGGCAAGAAAGTGC	TGGTTTCCTCCAACTCGCTG	188
AKT1	AGCGACGTGGCTATTGTGAAG	GCCATCATTCTTGAGGAGGAAGT	164
IL-6	ACTCACCTCTTCAGAACGAATTG	CCATCTTTGGAAGGTTCAGGTTG	149

Gene	Forward Primer Sequence (5'→3')	Reverse Primer Sequence (5'→3')	Product Length (bp)
TNF-α	CCTCTCTCTAATCAGCCCTCTG	GAGGACCTGGGAGTAGATGAG	220

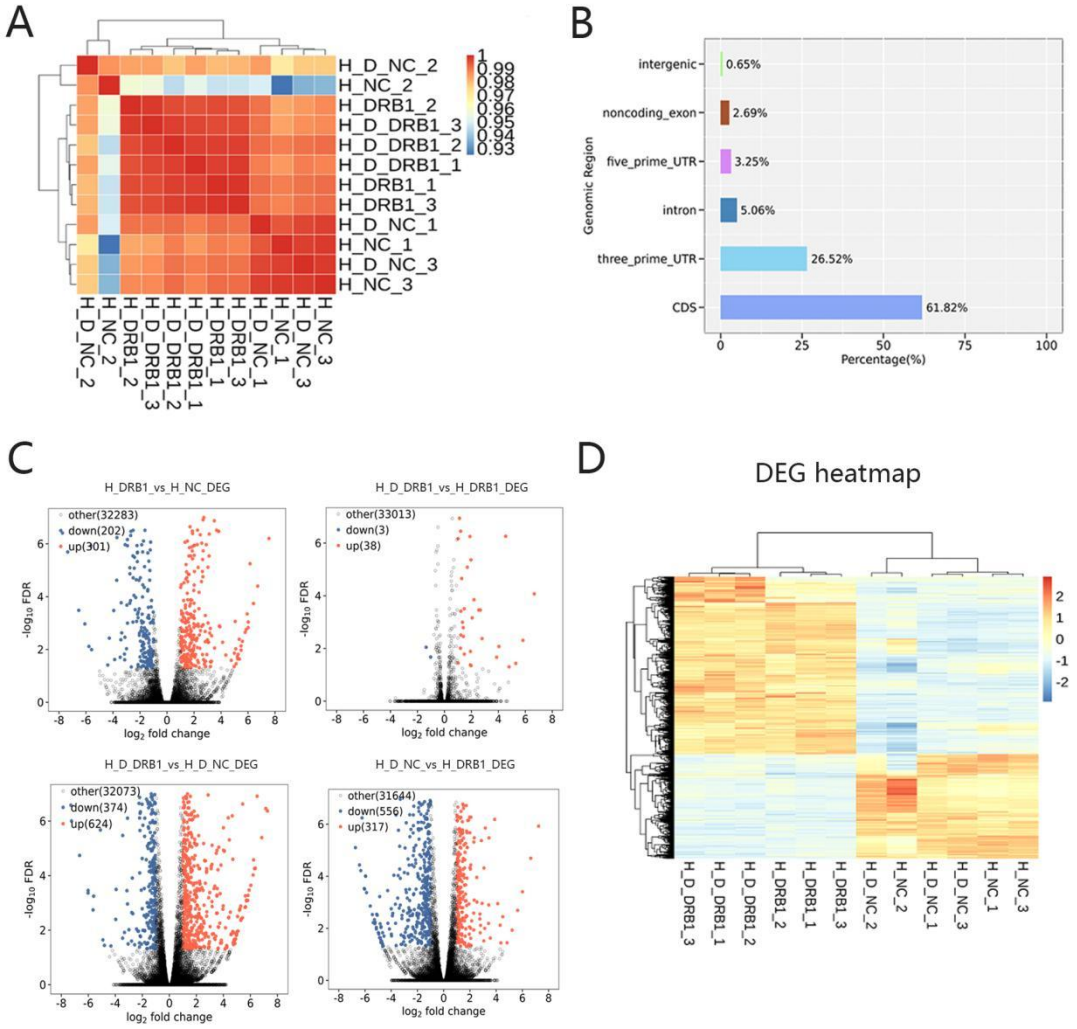


Fig 1 RNA-seq data quality assessment and analysis of differentially expressed genes (DEGs).

(A) Distribution of sequencing reads across coding sequences (CDS), 3′ untranslated regions (3′ UTR), 5′ UTR, and intergenic regions. (B) Heatmap of gene expression profiles across four groups of HUVECs: Control, high glucose (HG), HG + empty lentivirus (OE-NC), and HG + hsa-HLA-DRB1 overexpression lentivirus (OE-hsa-HLA-DRB1). Each column represents an individual biological replicate (n = 3). Red indicates high expression; blue indicates low expression. The Pearson correlation coefficient (r) between samples was ⩾ 0.92. (C) Bar chart and overlap analysis depicting the number of DEGs identified in pairwise comparisons among the four groups. DEGs were defined by $|\log_2(\text{fold change})| \geqslant 1$ and false discovery rate (FDR) < 0.05. The HG + OE-hsa-HLA-DRB1 group exhibited the highest number of DEGs (n = 998), with a 68.3% overlap with the control group.

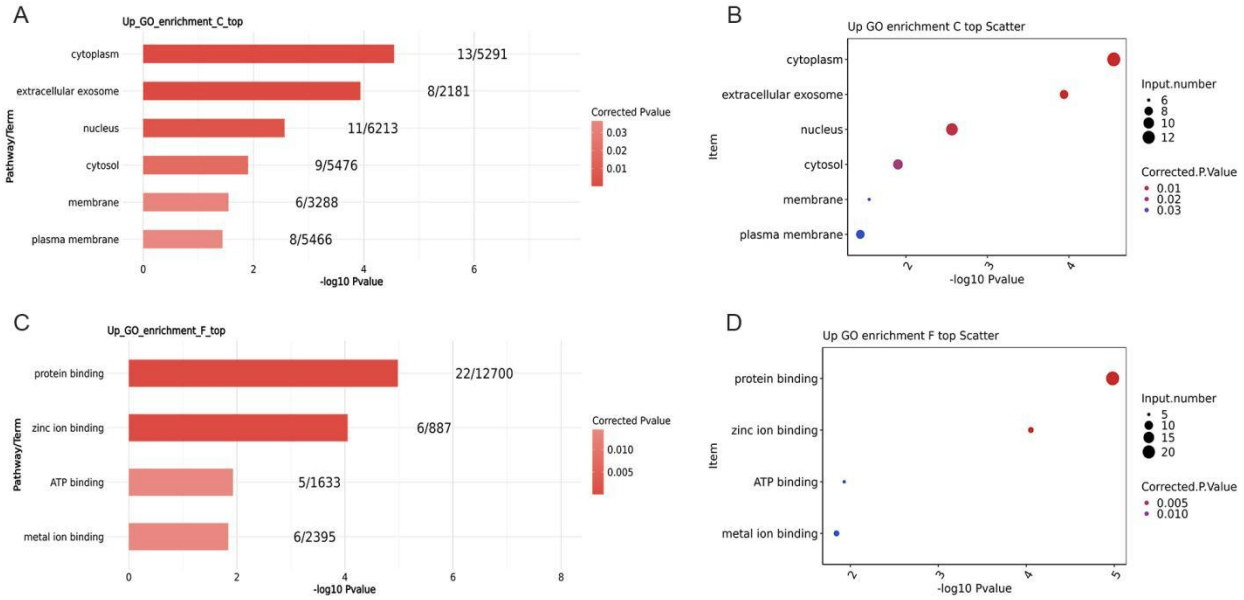


Fig 2 Gene Ontology (GO) enrichment analysis of differentially expressed genes.
(A) Scatter plot of enriched cellular component (CC) terms for upregulated DEGs. (B) Scatter plot of enriched molecular function (MF) terms for upregulated DEGs. (C) Bubble plot of enriched biological process (BP) terms for upregulated DEGs. (D) Bubble plot of enriched biological process (BP) terms for downregulated DEGs. The x-axis represents the $-\log_{10}$(adjusted P-value); the y-axis lists the enriched GO terms. The size of each bubble/dot corresponds to the number of enriched genes, and the color intensity reflects the significance of enrichment.

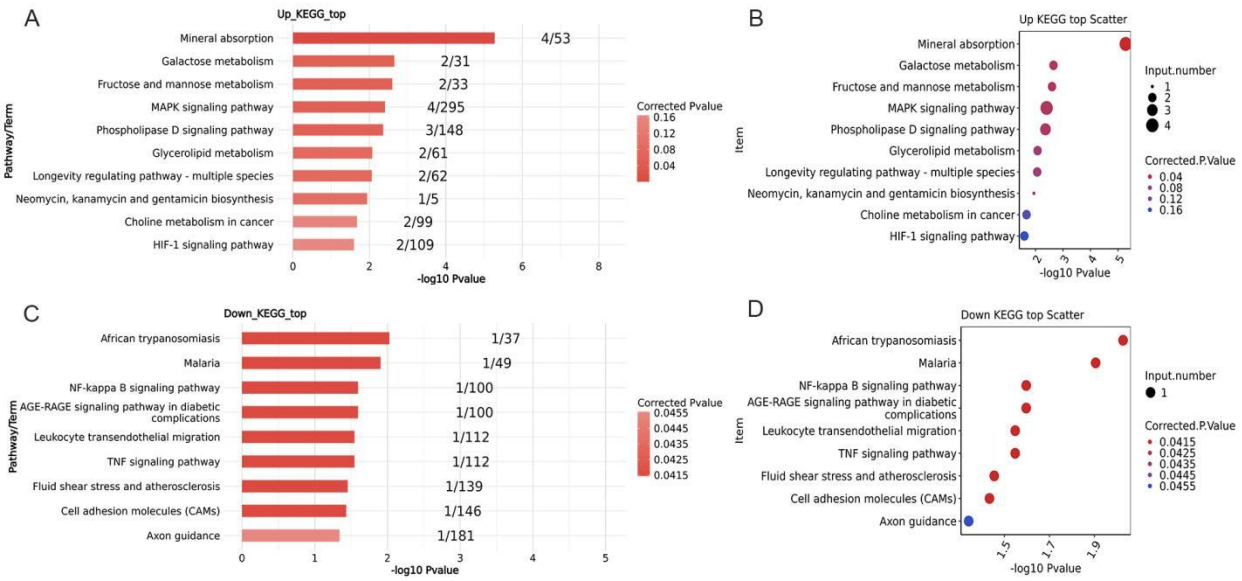


Fig 3 Kyoto Encyclopedia of Genes and Genomes (KEGG) pathway enrichment analysis of differentially expressed genes.
(A) Bubble plot of KEGG pathways enriched among upregulated DEGs. (B) Bubble plot of KEGG pathways enriched among downregulated DEGs. The x-axis represents the enrichment factor (GeneRatio); the y-axis lists the pathway names. The size of each bubble corresponds to the number of enriched genes, and the color gradient reflects the $-\log_{10}$(P-value), with darker colors indicating greater enrichment significance.

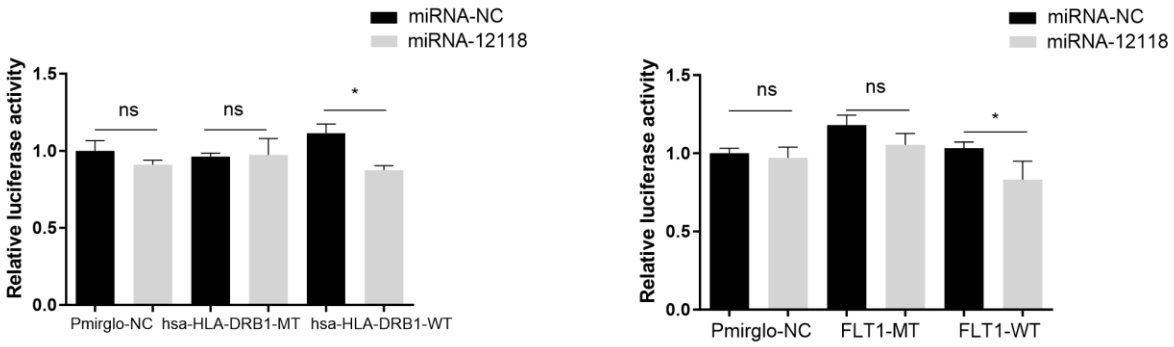


Fig 4 Validation of direct binding relationships within the hsa-HLA-DRB1/miRNA-12118/FLT-1 axis by dual-luciferase reporter assay.
Relative luciferase activity was measured in 293T cells co-transfected with wild-type (WT) or mutant (MUT) reporter vectors and miRNA-12118 mimics or a negative control (NC). A significant reduction in luciferase activity was observed in the WT + miRNA-12118 mimics group compared with the NC group (**P < 0.01), confirming the direct targeting interaction. Data are presented as mean ± SD (n = 3).

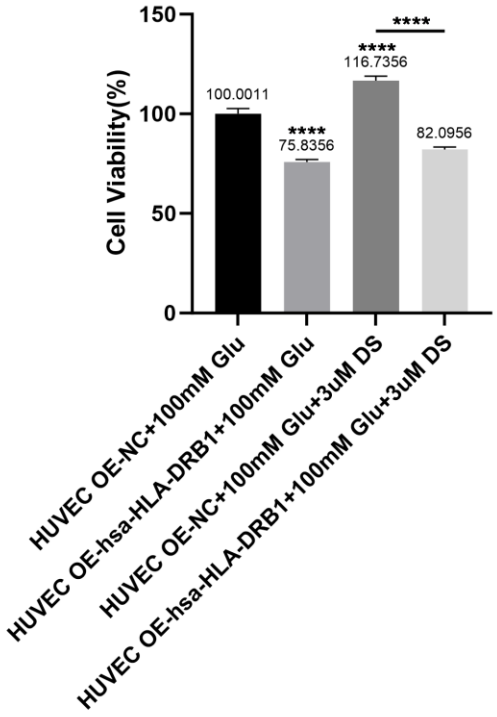


Fig 5 Effect of deoxyshikonin (DS) on the proliferation of hsa-HLA-DRB1-overexpressing HUVECs under high glucose conditions.

Cell viability was assessed using the CCK-8 assay in the following groups: Control, high glucose (HG), HG + empty lentivirus (OE-NC), HG + hsa-HLA-DRB1 overexpression (OE-hsa-HLA-DRB1), HG + 3 μmol/L DS (HG + DS), and HG + OE-hsa-HLA-DRB1 + DS. Compared with the Control group, cell viability was significantly reduced in the HG group (*P < 0.001). Compared with the HG group, cell viability was markedly elevated in the HG + OE-hsa-HLA-DRB1 group (*P < 0.001). Compared with the HG + OE-hsa-HLA-DRB1 group, cell viability was significantly decreased in the HG + OE-hsa-HLA-DRB1 + DS group (***P < 0.001). Data are expressed as mean ± SD (n = 3).

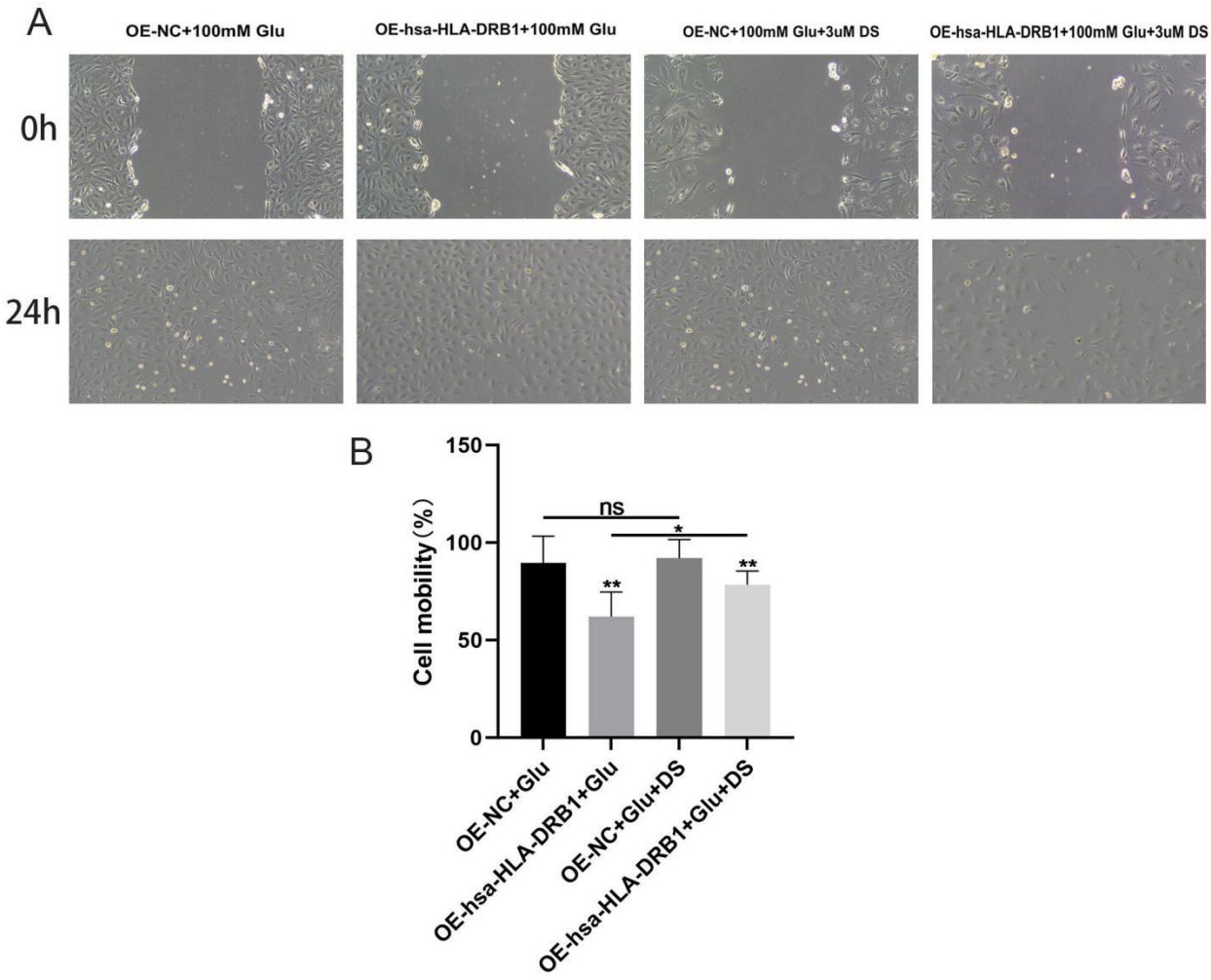


Fig 6 Effect of deoxyshikonin (DS) on the migratory capacity of hsa-HLA-DRB1-overexpressing HUVECs under high glucose conditions.
Cell migration was evaluated using the wound healing assay. (A) Representative images captured at 0 h and 21 h post-scratch (100× magnification). (B) Quantification of the cell migration rate. Compared with the HG group, the migration rate was significantly decreased in the HG + OE-hsa-HLA-DRB1 group (*P < 0.05). Compared with the HG + OE-hsa-HLA-DRB1 group, the migration rate was significantly increased in the HG + OE-hsa-HLA-DRB1 + DS group (*P < 0.05). Data are presented as mean ± SD (n = 3).

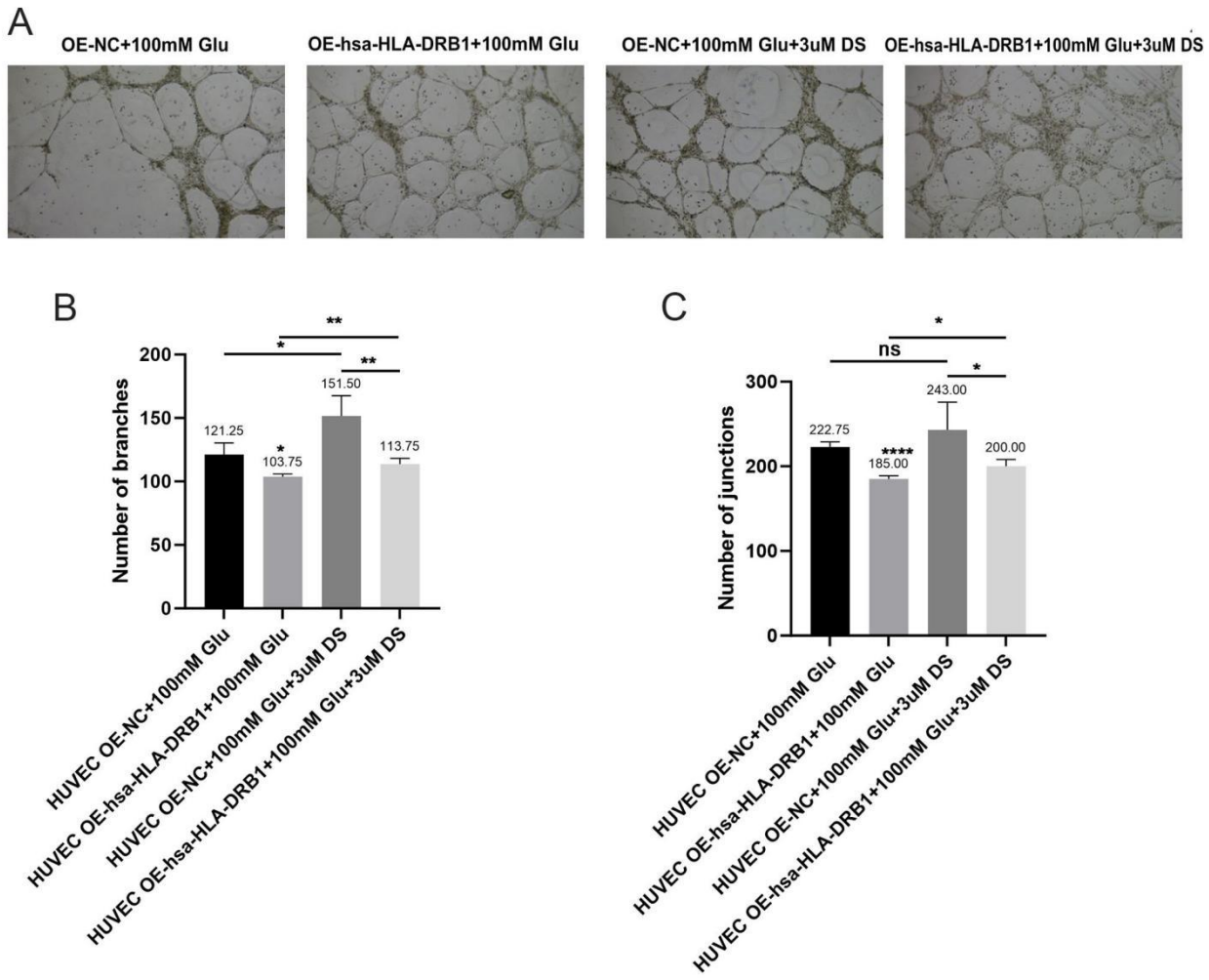


Fig 7 Effect of deoxyshikonin (DS) on the angiogenic capacity of hsa-HLA-DRB1-overexpressing HUVECs under high glucose conditions.
(A) Representative images of tube formation on Matrigel. (B) Quantification of the number of vascular branch points. (C) Quantification of the number of vascular junctions. Compared with the HG + OE-hsa-HLA-DRB1 group, *P < 0.05. Data are presented as mean ± SD (n = 3).

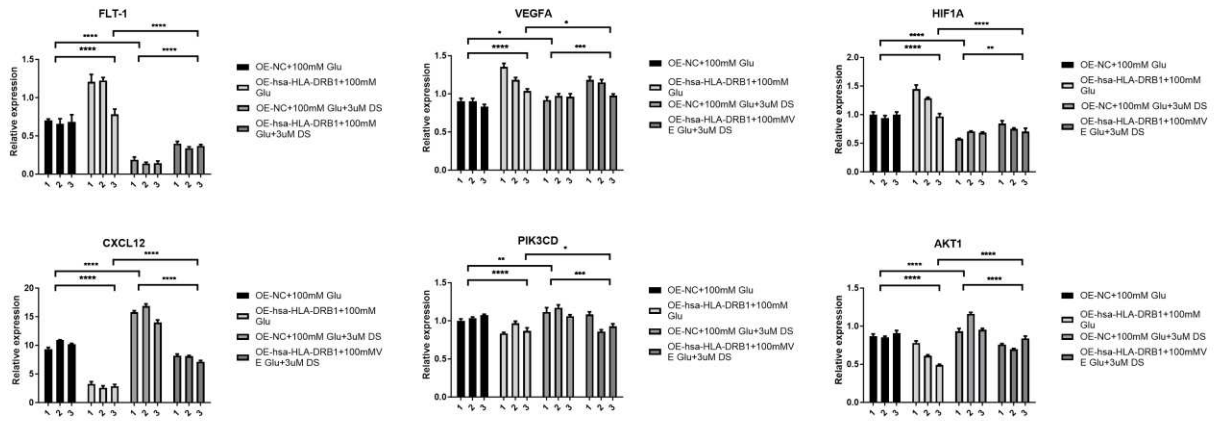


Fig 8 Deoxyshikonin (DS) modulates the mRNA expression of key downstream molecules in the hsa-HLA-DRB1 signaling pathway.
RT-qPCR analysis of relative mRNA expression levels in the indicated groups. Compared with the HG + OE-NC group, *P < 0.05, **P < 0.01, ***P < 0.001; compared with the HG + OE-hsa-HLA-DRB1 group, ***P < 0.001. Data are expressed as mean ± SD (n = 3).

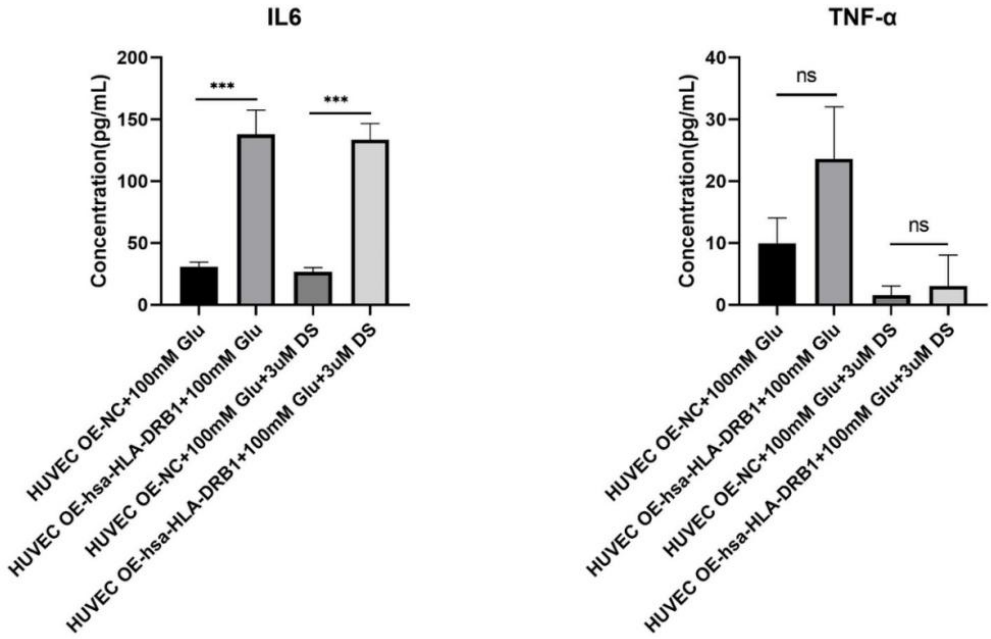


Fig 9 Effect of deoxyshikonin (DS) on the secretion of inflammatory cytokines in hsa-HLA-DRB1-overexpressing HUVECs under high glucose conditions.
Concentrations of IL-6 and TNF-α in cell culture supernatants were measured by ELISA. Compared with the HG + OE-NC group, the IL-6 concentration was significantly elevated in the HG + OE-hsa-HLA-DRB1 group (***P < 0.001). Compared with the HG + OE-hsa-HLA-DRB1 group, the IL-6 concentration was significantly reduced in the HG + OE-hsa-HLA-DRB1 + DS group (**P < 0.01). Data are presented as mean ± SD (n = 3).

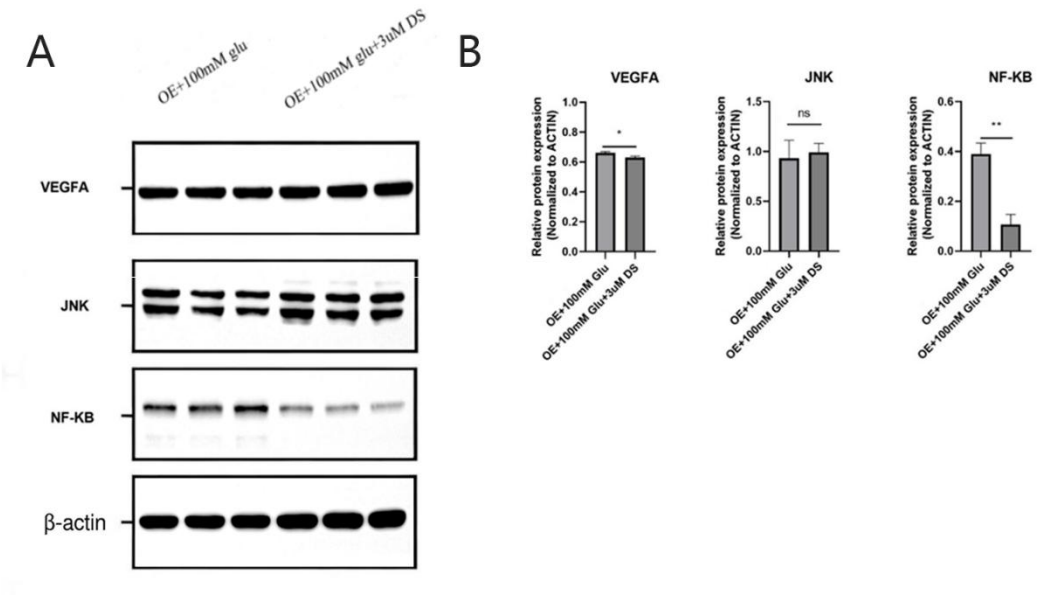


Fig 10 Effect of deoxyshikonin (DS) on the expression of related proteins in HUVECs under combined high glucose and hsa-HLA-DRB1 overexpression.
Western blot analysis of VEGFA, JNK, and NF-κB protein expression levels. β-actin was used as an internal loading control. (A) Representative immunoblot images. (B) Densitometric quantification of protein bands. Compared with the OE + 100 mmol/L Glu group, VEGFA expression was slightly decreased (0.78 ± 0.08 vs. 1.18 ± 0.10, *P < 0.05), NF-κB expression was significantly downregulated (0.52 ± 0.07 vs. 1.32 ± 0.13, **P < 0.01), and JNK expression showed no significant difference (*P* > 0.05) in the OE + 100 mmol/L Glu + 3 μmol/L DS group. Data are expressed as mean ± SD (n = 3).

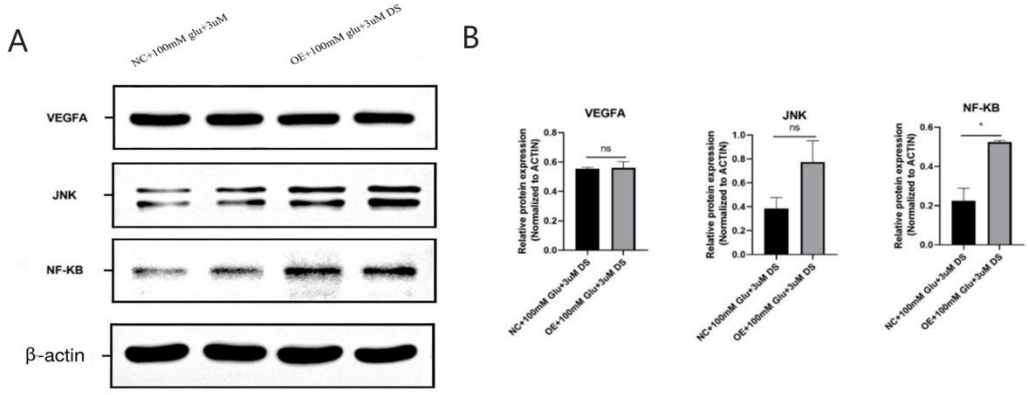


Fig 11 Effect of deoxyshikonin (DS) on VEGFA, NF-κB, and JNK protein expression in non-overexpressing and hsa-HLA-DRB1-overexpressing high glucose-induced HUVECs.
(A) Representative immunoblot images of VEGFA, NF-κB, and JNK. The groups are as follows: Control, high glucose (HG), HG + DS, HG + OE-hsa-HLA-DRB1, and HG + OE-hsa-HLA-DRB1 + DS. (B) Densitometric quantification of relative protein expression levels. β-actin served as an internal loading control. Compared with the HG group, the expression levels of VEGFA, NF-κB, and JNK were significantly decreased in the HG + DS group (*P < 0.05). Compared with

the HG + OE-hsa-HLA-DRB1 group, the expression levels of VEGFA, NF-κB, and JNK were significantly decreased in the HG + OE-hsa-HLA-DRB1 + DS group (**P < 0.01). Data are expressed as mean ± SD (n = 3).

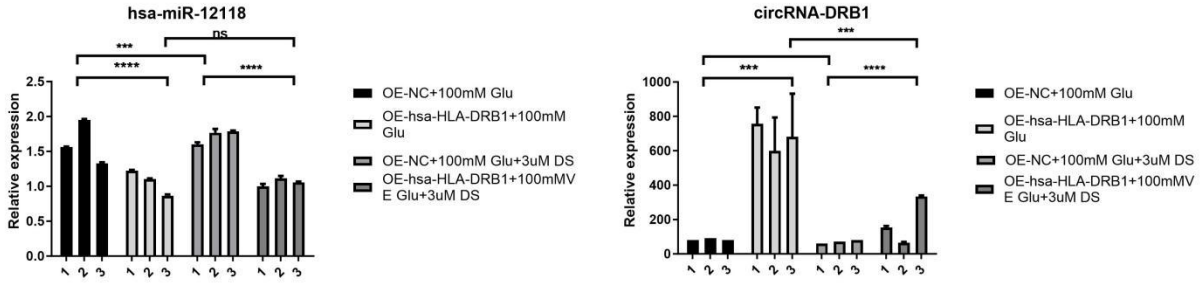


Fig 12 Deoxyshikonin (DS) regulates the hsa-HLA-DRB1/miRNA-12118 axis and its downstream target gene expression.
RT-qPCR analysis of relative miRNA-12118 expression levels in the indicated HUVEC groups. Compared with the OE-NC + 100 mmol/L Glu group, miRNA-12118 expression was significantly decreased in the OE-hsa-HLA-DRB1 + 100 mmol/L Glu group (0.35 ± 0.06-fold, ***P < 0.001). Following intervention with 3 μmol/L DS, miRNA-12118 expression was restored to 0.98 ± 0.10-fold (***P < 0.001). Data are presented as mean ± SD (n = 3).

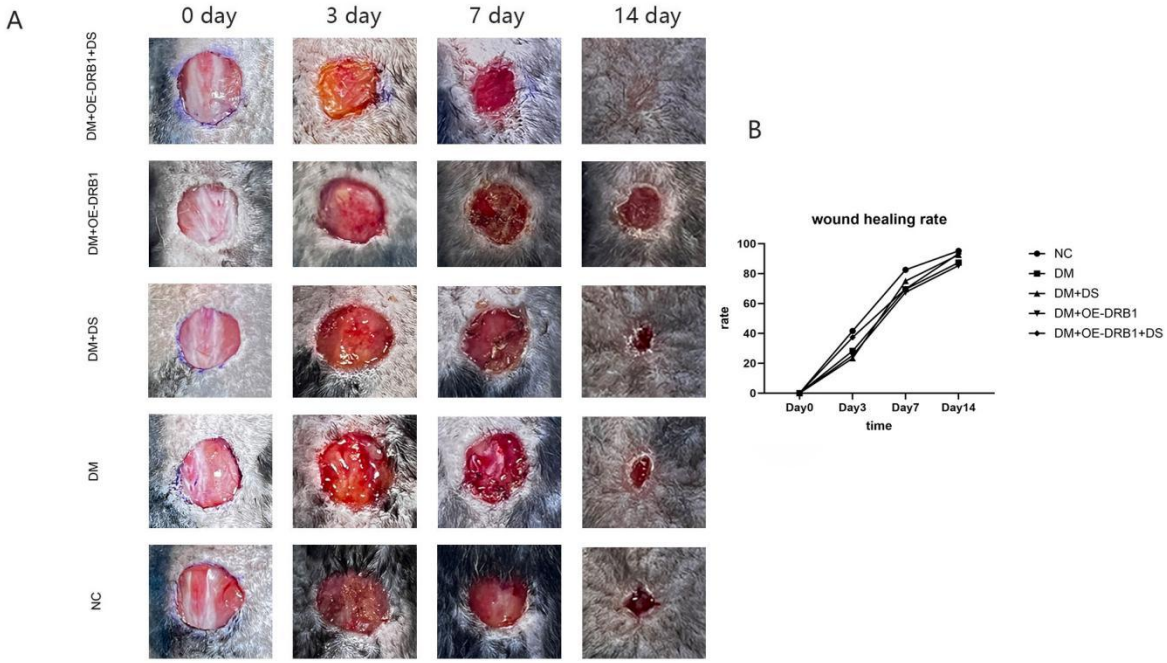


Fig 13 Effect of deoxyshikonin (DS) on wound healing rates in diabetic mice.
(A) Representative macroscopic images of wounds in each group at days 0, 3, 7, 10, and 14 post-wounding. (B) Quantitative analysis of wound healing rates over time. Compared with the DM group, **P < 0.01, ***P < 0.001; compared with the DM + OE-hsa-HLA-DRB1 group, ***P < 0.001. Data are expressed as mean ± SD (n = 7 per group).

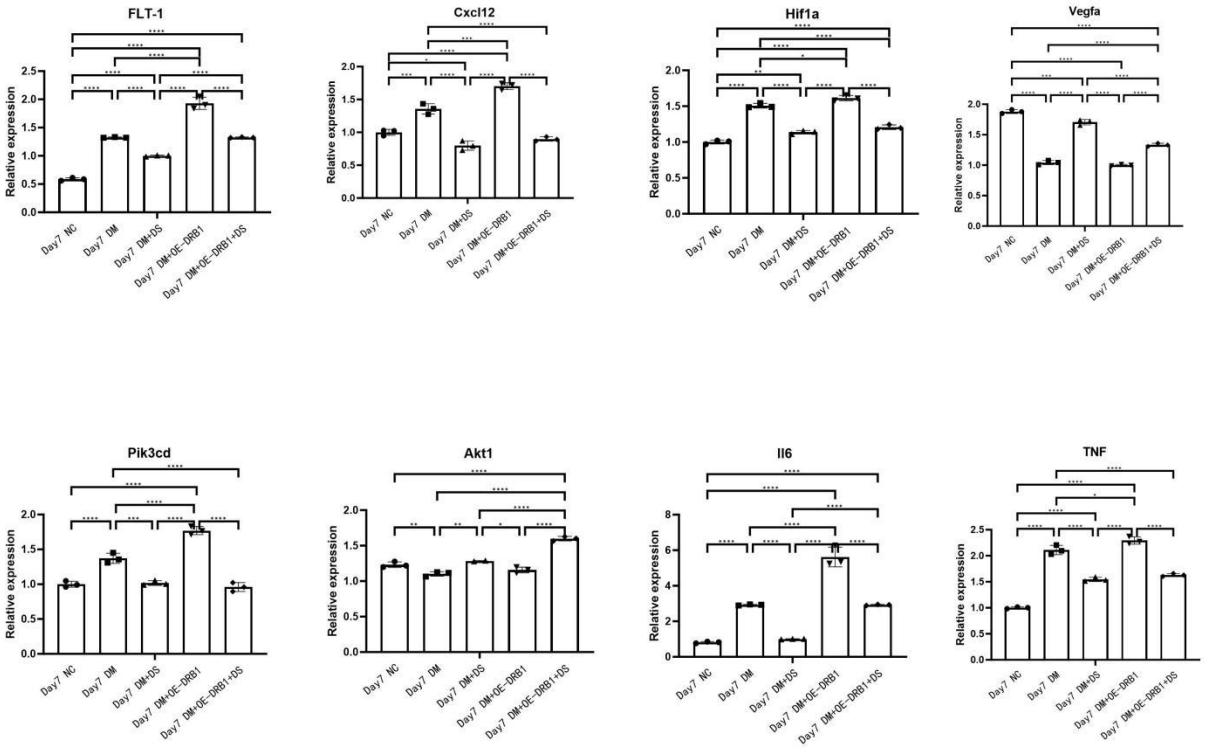


Fig 14 RT-qPCR analysis of HLA-DRB1/miRNA-12118 axis gene expression in wound tissue from diabetic mice on day 7 post-wounding.
Relative mRNA expression levels of HLA-DRB1, miRNA-12118, and FLT1 in wound granulation tissue. Compared with the DM group, ***P < 0.001; compared with the DM + OE-hsa-HLA-DRB1 group, ***P < 0.001. Data are presented as mean ± SD (n = 3 per group).

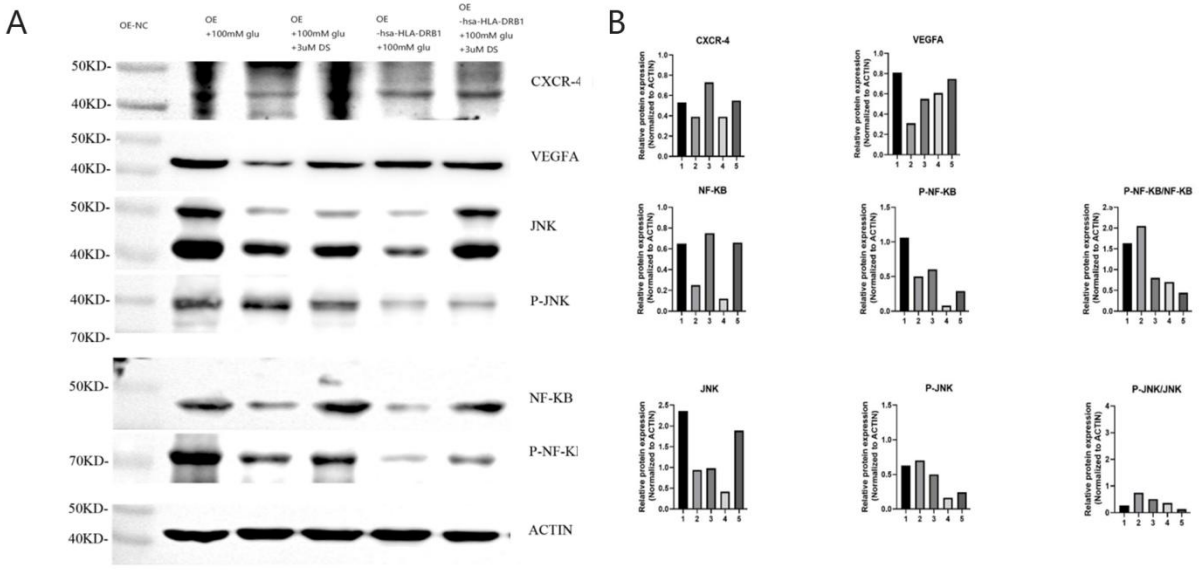


Fig 15 Western blot analysis of related protein expression in wound tissue from diabetic mice on day 14 post-wounding.

(A) Representative immunoblot images of JNK and NF-κB. β-actin was used as a loading control. (B) Densitometric quantification of protein expression levels. Compared with the DM group, ***P < 0.001; compared with the DM + OE-hsa-HLA-DRB1 group, ***P < 0.001. Data are expressed as mean ± SD (n = 3 per group).

Supplementary Files

This is a list of supplementary files associated with this preprint. Click to download.

- Westernblot.pdf
- KEGGPERMISSION261189.pdf